

CFD analysis of heat transfer within a bottom heated vertical concentric cylindrical enclosure

Asif Hussain Malik^{1,*}, Ajmal Shah² and Shahab Khushnood¹

¹ Department of Mechanical Engineering, University of Engineering and Technology, Taxila, Pakistan

² Department of Mechanical Engineering, Pakistan Institute of Engineering and Applied Sciences, Nilore, Islamabad, Pakistan

* Corresponding e-mail address: asifhussainmalik@yahoo.com

Abstract

The CFD analysis of heat transfer within a bottom heated vertical concentric cylindrical enclosure is important with respect to the process in the chemical and process industries. The research work focuses on the CFD analysis of the enclosure with respect to the machines used for the segregation of chemicals in the chemical industries. The CFD simulations are performed to study the effects of inner cylinder material and outer cylinder geometric configurations on the heat transfer mechanism in the enclosure. The CFD simulations are conducted at a bottom disc temperature of 393 K and compared with the published results at a temperature of 433 K. This research study depicts the behavior of bottom heated vertical concentric cylindrical enclosure at different bottom disc temperatures. This study also investigates the heat transfer mechanism of the enclosure using different inner cylinder materials and different configurations of the outer cylinder. In such enclosures a uniform temperature is required for the segregation of chemicals. A more uniform temperature is observed in the enclosure by using aluminum inner cylinder of the bottom disc and using two different diameter outer cylinders as compared to the mild steel and stainless steel.

Keywords: CFD simulations, heat transfer, enclosure, temperature,

1. Introduction

The past researchers studied heat transfer through cylindrical enclosures in the last couples of decades. It has many engineering applications in building machines, solar collectors, heat exchangers, materials processing, storage tanks, furnace designs and nuclear designs.

The past researchers conducted numerical study of heat transfer using different enclosures. Lemembre and Petit [1] numerically investigated two-dimensional laminar natural convection heat transfer in cylindrical enclosures of heated lateral walls at uniform heat flux and cooled at the same heat flux at the top surface by insulating the bottom surface. The convection heat transfer was enhanced with the increase of aspect ratio and Rayleigh number. Chen, Ho and Humphrey [2] numerically presented two-dimensional steady-state laminar natural convection in the rectangular enclosures. The flow and heat transfer in the enclosure were strongly affected by an asymmetric specification of side wall temperatures. The asymmetry induced a disproportionately rise in the Nusselt number of the hotter side wall relative to the decrease in Nusselt number of the colder wall. References [3-6] numerically investigated the convection heat transfer in the cylindrical enclosures with thermo-physical fluid properties assumed to be constant except density variation which varies according to Boussinesq approximation.

Kim and Viskanta [7] and Vargas et al. [8] presented the experimental and numerical study of steady natural convection in two-dimensional Newtonian and incompressible fluid-filled enclosures. They concluded that heat conduction reduced average temperature difference across the enclosure, partially stabilized the flow ultimately decreasing natural convection heat transfer. The heat transfer and fluid flow



leading to thermal stratification inside the enclosure were also studied. Kee et al. [9] presented experimental and numerical study of steady natural convection of a heat generating tritium gas in a two-dimensional closed vertical cylinders and spheres with their bounding isothermal walls. They demonstrated experimental and analytical agreement for local temperatures over a range of Grashof numbers. Bohn and Anderson [10] experimentally investigated heat transfer between parallel and perpendicular vertical walls in a three-dimensional water-filled cubical enclosure with an adiabatic top and bottom and isothermal sides and discussed many aspects of natural convection flow.

Liaquat and Baytas [11] numerically analyzed laminar two-dimensional conjugate natural convection in an enclosure. Their research has shown a significant change in the buoyancy flow parameters as compared to convectional non-conventional investigations. Sharma et al. [3] numerically investigated the conjugate transient natural convection in a liquid sodium filled cylindrical enclosure with internal volumetric heat generating source. The lateral walls of the enclosure were isothermal, while the top and bottom walls were adiabatic. They presented the transient features of confined turbulent natural convection due to time varying generation of heat in the volumetric source and shown that the intensity of heat source exponentially decayed with time. Kuznetsov and Sheremet [12] numerically investigated the two-dimensional conjugate convective-conductive heat transfer in a rectangular enclosure due to the local heat and contaminant sources and convective radiative heat exchange with an environment. The effects of Grashof number, buoyancy ratio and transient factor on flow modes, heat and mass transfer are studied. Glakpe et al. [13] numerically investigated the laminar, three-dimensional natural convection in the air-filled vertical annular space formed by a square rod enclosed within a cylinder strongly affected by the Rayleigh number. They studied the effects of thermal radiation exchange between walls of an enclosure.

This research paper presents thermal behavior of the system, adjusts the cooling system as per requirements, gives insight of different configurations and promotes the understanding of natural convection heat transfer between two concentric cylinders and gives special attention to the material study not yet performed previously as per authors' knowledge.

2. Experimental set up

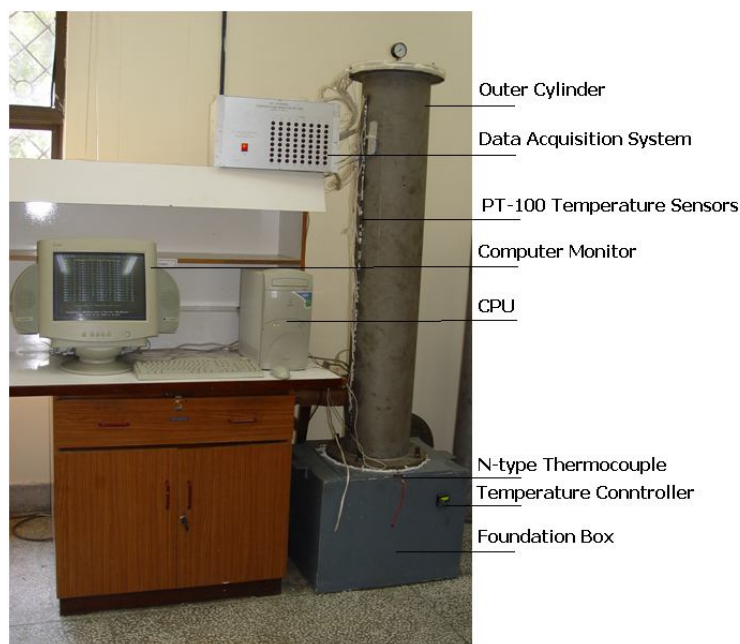


Figure 1: Experimental Apparatus

In this research paper, the CFD analysis of heat transfer within the bottom heated vertical concentric cylindrical enclosure (Figure 1) is numerically investigated at a specified bottom disc temperature of

393 K at the top centre of the bottom disc using two different configurations with three different materials of the inner cylinders and discs and compared with the published results at a temperature of 393 K [14]. Thermal analyses of the inner cylinders materials and two geometric configurations of enclosure (with aspect ratios $A_1 = 6.016$ and $A_2 = 5.133$ and Radius ratios $RR_1 = 1.753$ and $RR_2 = 2.055$ respectively) are performed.

3. Mathematical formulation

Mathematical formulation of the buoyancy flow effects in the fluid-filled enclosures includes the governing equations of conservation of mass, momentum and energy to solve the flow domain. To deal with the conduction within the solids and radiations from hot surfaces their mathematical formulation must be added. In the subsequent articles a brief introduction of the equations necessary for solving conjugate heat transfer processes is given.

The Navier-Stokes governing equations in their differential form in 2-D cylindrical coordinate system (r, z) can be written as under:

$$\frac{\partial \rho}{\partial t} + \frac{\partial}{\partial z}(\rho v_z) + \frac{\partial}{\partial r}(\rho v_r) + \frac{\rho v_r}{r} = S_m \quad (1)$$

$$\frac{\partial}{\partial t}(\rho v_z) + \frac{1}{r} \frac{\partial}{\partial z}(r \rho v_z v_z) + \frac{1}{r} \frac{\partial}{\partial r}(r \rho v_r v_z) = -\frac{\partial p}{\partial z} + \frac{1}{r} \frac{\partial}{\partial z} \left(r \mu \left\{ 2 \frac{\partial v_z}{\partial z} - \frac{2}{3} (\nabla \cdot \mathbf{v}) \right\} \right) + \frac{1}{r} \frac{\partial}{\partial r} \left(r \mu \left\{ \frac{\partial v_z}{\partial r} + \frac{\partial v_r}{\partial z} \right\} \right) + F_z \quad (2)$$

$$\frac{\partial}{\partial t}(\rho v_r) + \frac{1}{r} \frac{\partial}{\partial z}(r \rho v_z v_r) + \frac{1}{r} \frac{\partial}{\partial r}(r \rho v_r v_r) = -\frac{\partial p}{\partial r} + \frac{1}{r} \frac{\partial}{\partial z} \left(r \mu \left\{ 2 \frac{\partial v_r}{\partial z} + \frac{\partial v_z}{\partial r} \right\} \right) + \frac{1}{r} \frac{\partial}{\partial r} \left(r \mu \left\{ 2 \frac{\partial v_r}{\partial r} - \frac{2}{3} (\nabla \cdot \mathbf{v}) \right\} \right) - 2 \mu \frac{v_r}{r^2} + \frac{2}{3} \frac{\mu}{r} (\nabla \cdot \mathbf{v}) \rho \frac{v_z^2}{r} + F_r \quad (3)$$

The stress tensor $\boldsymbol{\tau}$ is given by;

$$\boldsymbol{\tau} = \mu [(\nabla \mathbf{v} + \nabla \mathbf{v}^T) - \frac{2}{3} \nabla \cdot \mathbf{v} \mathbf{I}] \quad (4)$$

$$\frac{\partial}{\partial t}(\rho E) + \nabla \cdot (\mathbf{v}(\rho E + p)) = \nabla \cdot (k_{eff} \nabla T - \sum_j h_j \mathbf{J}_j + (\boldsymbol{\tau}_{eff} \cdot \mathbf{v})) + S_h \quad (5)$$

Where, r = radial coordinate, z = axial coordinate, v_r = radial velocity of the fluid, v_z = axial velocity of the fluid, ρ = density of fluid, S_m = mass source term within the differential volume, p = static pressure, $\boldsymbol{\tau}$ = stress tensor, \mathbf{g} = acceleration due to gravity, \mathbf{F} = external body forces including other model-dependent source terms such as porous medium and user-defined sources, μ = dynamic viscosity, \mathbf{I} = unit tensor, k_{eff} = effective conductivity including the effect of turbulent thermal conductivity \mathbf{J}_j = diffusion flux of species, and j . $\boldsymbol{\tau}_{eff}$ = effective stress tensor, S_h = energy source term including radiation source, chemical reaction source etc.

These equations (1-5) are given in detail in [15-18]. The first three terms on the right side of Eq. 5 give energy transfer due to conduction, species diffusion and viscous dissipation, respectively. The buoyancy forces can be designated by the ratio of Grashof and Reynolds numbers as shown below;

$$\frac{Gr}{Re^2} = \frac{g \beta \Delta T L}{v^2} \quad (6)$$

There are strong buoyancy effects on the fluid flow when the above number approaches or exceeds unity. The strength of the buoyancy-induced flow in the pure natural convection is measured by the Rayleigh number;

$$Ra = \frac{g \rho \beta \Delta T L^3}{\mu \alpha} \quad (7)$$

Where, β = coefficient of thermal expansion and α = thermal diffusivity.

$$\alpha = \frac{k}{\rho c_p} \quad (8)$$

A buoyancy-induced laminar flow is assumed at $Ra < 10^8$ and transition from laminar to turbulence is assumed in the range of $10^8 < Ra < 10^{10}$.

According to the Boussinesq approximation the density of the fluid is given by;

$$\rho = \rho_o[1 - \beta(T - T_o)] \quad (9)$$

Where, ρ_o = constant density of the fluid in the closed domain, T_o = operating temperature and β = coefficient of thermal expansion.

Fourth term of the energy equation (Eq. 5) (S_h) also includes the heat source due to radiation. Rosseland radiation model is used which is faster and requires less memory as compared to other radiation models and deals with axisymmetric geometries and contains the effect of scattering. The radiative heat flux equation, the equation becomes;

$$q_r = -16\sigma T^3 \nabla T \quad (10)$$

Both the specific radiative (q_r) and specific conduction heat fluxes (q_c) have the same form, therefore, these can be written as,

$$q = q_c + q_r = -(k + k_r) \nabla T \quad (11)$$

Where, k is the thermal conductivity, k_r is the radiative conductivity.

2.1 Boundary conditions

Appropriate boundary conditions are required to solve the Navier-Stokes equations. Boundary conditions are derived from the known parameters available at different physical boundaries of the domain as shown in Figure 2. The top and bottom walls of the enclosure are insulated (adiabatic), except the bottom disc, which act as a heat source for the enclosure. No slip boundary conditions are enforced at these walls of the enclosure. The outer side of the outer cylinder wall is exposed to natural convection at ambient conditions. The mathematical formulation of these boundary conditions is given below;

3.1.1. Bottom disc wall boundary

Heat source is applied at the bottom of the disc of radius, r_1 . N-type thermocouple probe is mounted at the upper central location of the bottom disc and connected to the temperature controller. The temperatures are specified for different experiments at $z = 0$ and known. Its boundary conditions are given below;

At $z = 0$; $0 < r < r_1$;

T is known; $v_r = v_z = 0$ (No slip condition);

3.1.2 Bottom insulated wall boundary

Bottom surface of enclosure is assumed to be insulated except the bottom disc heated by the heat source. Neither heat is entered into the bottom insulated wall nor does it come out of that wall. Its boundary conditions are given below;

At $z = 0$; $r_1 < r < r_2$;

$v_r = v_z = 0$ (No slip condition);

$q_{in} = q_{out} = 0$ for an adiabatic wall.

3.1.3 Side wall boundary

At the side wall of enclosure the natural convection heat transfer coefficient h_o is taken as a boundary of enclosure. Heat entering from the hot bottom disc after passing through the walls of inner cylinder comes out of the wall of outer cylinder of enclosure. Its boundary conditions are given below;

At $r = r_2$; $0 < z < z_2$;

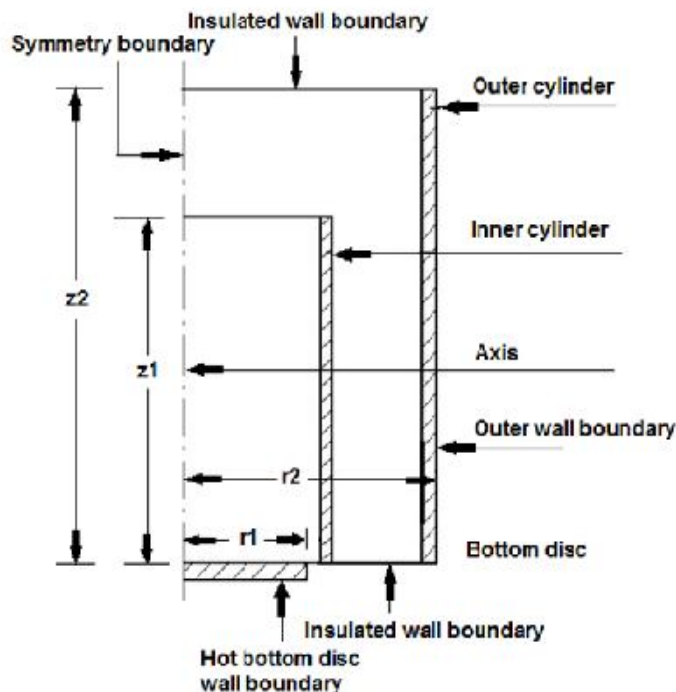


Figure 2: Boundary conditions of vertical concentric cylindrical enclosure

3.1.4 Symmetry boundary

In 2-D axisymmetric geometry the axis is used as a symmetry boundary and half of the geometry is taken for the analysis as shown in Figure 2 as used by the past researchers [1-5]. At the axis as a boundary conditions all the gradients of temperature and velocity are zero. Its boundary conditions are given below;

$$\text{At } r = 0; 0 \leq z < z_2;$$

$$\frac{\partial T}{\partial r} = 0; \frac{\partial v_z}{\partial r} = 0; \frac{\partial v_r}{\partial r} = 0;$$

3.1.5 Top insulated wall boundary

Top wall of enclosure is taken as insulated or adiabatic one. Neither heat is entered into the bottom insulated wall nor does it come out of that wall. Its boundary conditions are given below;

$$\text{At } z = z_2; 0 \leq r < r_2;$$

$$v_r = v_z = 0 \text{ (No slip condition);}$$

$$q_{in} = q_{out} = 0 \text{ for an adiabatic wall.}$$

4. Numerical analysis

In this research work the CFD analysis of the experimental work [19] depicting heat transfer effects within the bottom heated vertical concentric cylindrical enclosure (Figures 1 and 3) in the bottom disc temperature range of 393 K at the upper centre of the bottom disc is performed. This analysis provided a thorough insight of the flow and buoyancy effects due to the change of inner cylinder wall material in the enclosure and outer cylinder diameter. FLUENT 6.3 software is used to study the heat, mass and momentum transfer mechanisms within the enclosure, compare and validate numerical results with the experimental ones and get insight of the flow and thermal energy enhancement mechanism within the enclosure as used by the past researchers [8, 19-20].

Two dimensional steady state analysis is carried out. The Rosseland radiation model is selected. Air is treated as a stationary, incompressible and laminar fluid.

The FLUENT have used the pressure-based solver, the second order scheme is used for pressure, while the second order upwind discretization schemes are used for momentum and energy [21]. The

flow and energy equations are solved by the FLUENT [15] and the Green-Gauss cell-based gradient scheme is selected for this research work. Boussinesq approximation is used assuming the density as a constant, except in the buoyancy term of vertical momentum equation. In order to solve the pressure-velocity coupling SIMPLE algorithm is used as applied by the previous researchers [3, 6, 22-26]. The convergence criteria are different for different cases as shown in the previous studies by [27-29]. Iterations took place till the convergence is achieved to the required solution in the range of 765 ~ 4968 iterations. Three different materials of inner cylinders and discs in the enclosure are used in the analysis. Six experiments are performed at the specific temperatures of 393K on the upper central location of bottom discs. The mesh selected is square and total cells of both configurations (O_1 and O_2) are 213960 and 247400 respectively.

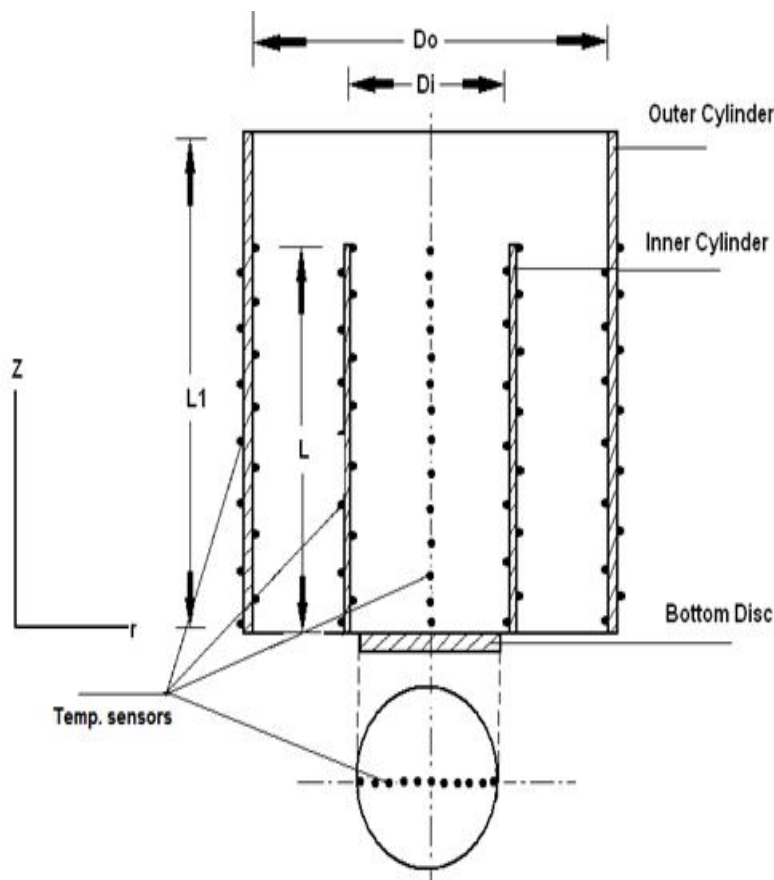


Figure 3: Cross-sectional view of concentric cylindrical enclosure

4.1 Geometry and meshing

In this research work the geometry considered for analysis is a 2-D axisymmetric one due to which the axis is used as a symmetry boundary. The half of the geometry is taken for the analysis due to its axisymmetric geometry as used by the past researchers [3, 19, 30-32]. Gambit 2.3.16 has been used as a preprocessor to construct the geometry and mesh.

The geometry is generated and meshed in the Gambit software as shown in the Figure 4. Square mesh is used to mesh the geometry. Along the axis of the geometry there are 1541 grid points, while at the top and bottom of the geometry there are 211 grid points. Due to change in diameters of the radial grid are 139 and 151 for outer cylinder, O_1 & O_2 respectively. The thermal energy enhancement about the axis of the geometry is assumed symmetric. Two-dimensional axisymmetric simulations are carried out. The bottom disc geometry of the enclosure being simulated is shown in the Figure 2. Top and bottom walls of the enclosure except the bottom disc are assumed to be adiabatic with no heat

flux and no heat generation. No slip condition is considered for all walls of the enclosure. The walls within the enclosure are thermally coupled.

The convection heat transfer coefficient, h is selected as a boundary condition at the outer surface of the outer vertical cylinder by hit and trial method. The inner and outer cylinders walls are considered as conducting walls. The user defined function has incorporated the experimental temperature results of bottom disc and coupled with the FLUENT [15]. The three inner cylinders of aluminum, mild-steel and stainless-steel having similar dimensions are used in different configurations.

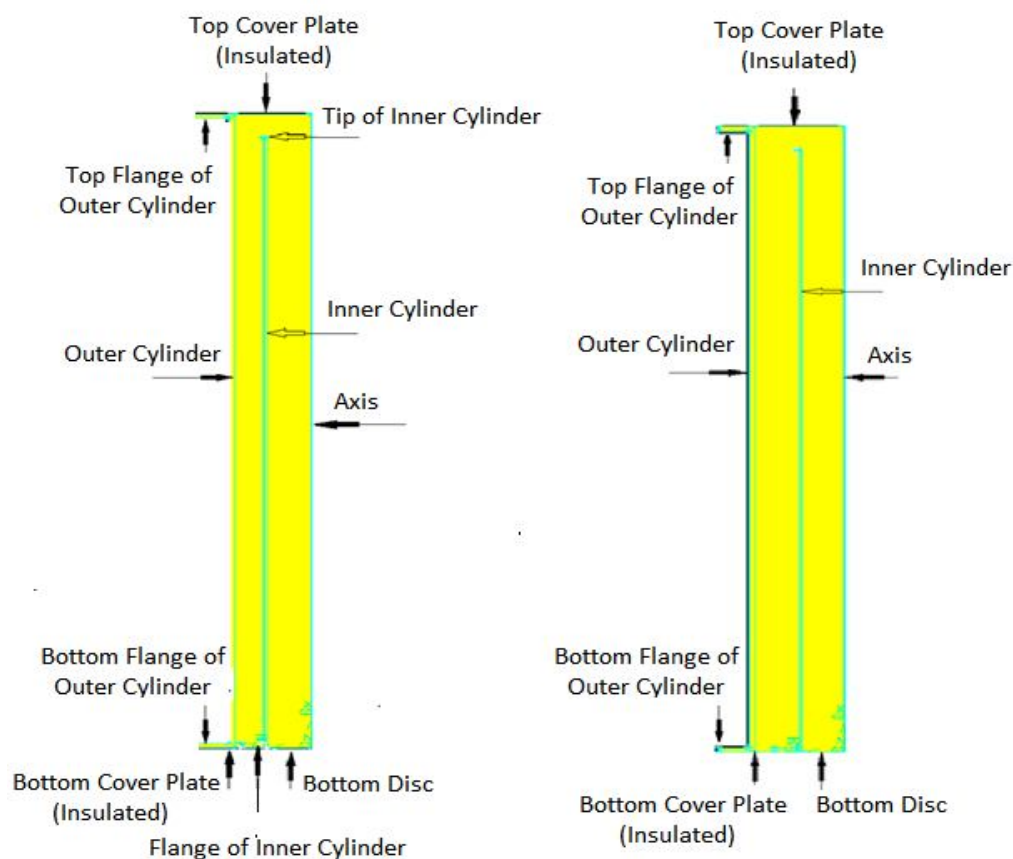


Figure 4: Meshing of enclosure geometries of outer cylinder, O_1 & O_2 outer cylinder

The outer surface of the simulated enclosure is far away from heat source, it was assumed that the pressure and temperature at the outer surface of the enclosure are equal to the ambient to allow free movement across this surface. There is an ambient temperature at the top of the vertical enclosure, so

Table 1: Properties of Fluid (Air)

Properties	Air
Density, kg/m^3	1.184
Specific heat capacity, J/kg.K	1007
Thermal conductivity, W/m.K	0.02551
Dynamic viscosity, Pa.sec	1.8949E-5
Absorption coefficient, $1/\text{m}$	0.49919, constant
Scattering phase function	Isotropic
Scattering coefficient, $1/\text{m}$	0
Thermal Expansion Coefficient, $1/\text{K}$	0.0033445
Refraction	1

Table 2: Properties of Materials

Properties	Aluminum	Mild Steel	Stainless Steel
Density, kg/m ³	2739	7833	8238
Specific heat capacity, J/kg.K	896	502	468
Thermal conductivity, W/m.K	222	45.3	13.4

Table 3: Geometric configurations of cylindrical enclosure

Parts of Geometry	Material	Diameter (m)	Thickness (m)	Height (m)
Bottom disc	Aluminum, Mild steel, Stainless steel	0.138	0.004	-
Inner cylinder	Aluminum, Mild steel, Stainless steel	0.146	0.005	1.48
Outer cylinder	Mild steel	O ₁ =0.256, O ₂ =0.300	0.01	1.54

the enclosure was assumed as an infinite enclosure. The properties of fluid (air) and materials [33] used in these simulations are given in the Tables 1 and 2 respectively.

4.2 Grid independence study

The grid independence study is carried out by taking the grids of cell sizes 2 mm, 1.5 mm, 1 mm and 0.5 mm having 54260, 96135, 213960 and 855840 cells with percentage errors of 4.2, 2.9, 1.94 and 1.91 respectively. There is a prominent percentage error of cell sizes 2 mm, 1.5 mm and 1 mm, while cell sizes 1 mm and 0.5 mm have almost the same percentage error with the experimental results of [14]. Therefore, cell size of 1 mm is taken while meshing the enclosure under research.

4.3 Uncertainty analysis

Experimental measurements always contain some uncertainties in spite of using high precision measuring instruments. Such uncertainties come from the measuring instrument, the items being measured, the environment, the operator and many other sources. The researchers generally estimate such uncertainties by using statistical method presented by Moffat [34]. In this study the same method is used to estimate the uncertainties in experimental data.

The N-type thermocouple used for measuring the temperature at the center of bottom disc has an accuracy of $\pm 0.75\%$, whereas, PT-100 temperature sensor has an accuracy of $\pm 0.3\%$. The temperature controller 'CAL Series 9900' and contactor (solid state relay) have accuracies of $\pm 0.25\%$ and $\pm 0.5\%$, respectively. The uncertainty in the reading of N-type thermocouple is estimated to be less than 1.5% and that of PT-100 temperature sensor it is 1.1%, including the effect of the observed experimental data scatter.

5. Results and discussion

This research work also includes the study of effect of outer cylinder diameter on the heat transfer within the enclosure. The numerical analysis is carried out using Fluent code. Numerical simulation

results of vertical concentric cylindrical enclosure are validated by comparing with the experimental data.

Thermal conductivity of inner cylinder material is thought to play a key role in affecting thermal behavior within the enclosure. For the material analysis three inner cylinders made of aluminum, mild steel and stainless steel are used. Thermal conductivity of aluminum is about 17 times greater than that of stainless steel and about 5 times greater than mild steel. To understand the heat transfer mechanism and buoyancy effects within the enclosure, the study of CFD results is required.

5.1 Axial thermal behavior

The temperature distribution along the axis and inner cylinder wall are very important to study the thermal behavior within the enclosure. The experimental and CFD results of axial temperature along the axis and inner cylinder of the enclosure are shown in Figures 6.1 and 6.2 respectively. The axial temperature distribution at axis of the geometry and inner cylinder are discussed in detail in the following articles.

5.1.1 Axis of the enclosure

Thermal behavior at the axis of enclosure gives true picture of heat transfer mechanism within the enclosure. The segregation of chemicals in the segregation machines takes place around the axis of the geometry and strongly depends on the thermal behavior along the axis.

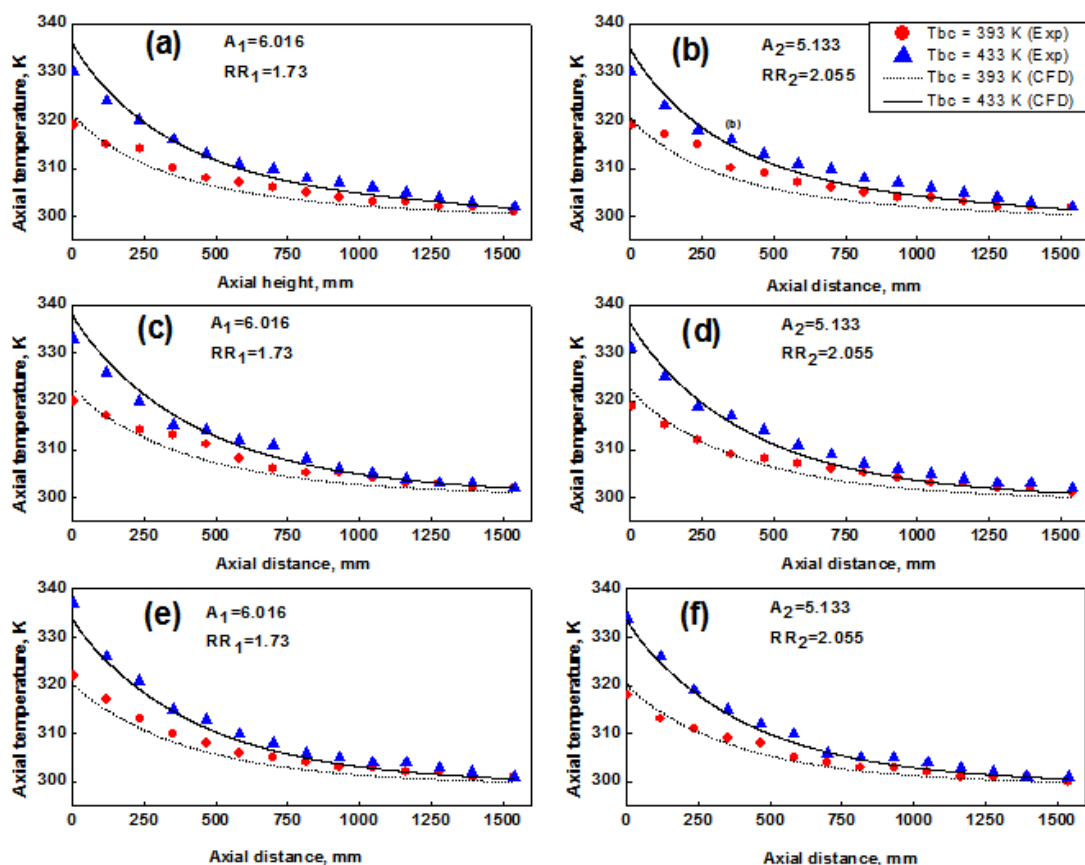


Figure 5: Axial temperature distribution along the axis of the enclosure with inner cylinder of aluminum (a, b), mild steel (c, d) and stainless steel (e, f).

Temperature at the axis is studied at bottom disc central temperature of 393 K, using inner cylinders of different materials (aluminum, mild steel and stainless steel) and outer cylinders of different diameter (O_1 and O_2) at bottom disc central temperature of 393 K as shown in Figure 5. The

experimental and numerical results of axial temperature match closely with each other for these six different cases and therefore validate the numerical simulations. The aspect ratio and radius ratio of the enclosure geometry with outer cylinder O_1 are 6.016 and 1.73, while with outer cylinder O_2 these values are 5.133 and 2.055 respectively.

The axial temperature decreases along the height of the enclosure for all the experiments performed due to the presence of heat source at the bottom of the enclosure. Figure 5 (a-b) shows that the axial temperature distribution is almost independent of the outer cylinder diameter. While, Figure 5 (c-f) shows that the axial temperature distribution is a function of the outer cylinder diameter especially at higher temperatures of the bottom disc. This response might be due to high thermal conductivity of aluminum as compared to mild steel and stainless steel.

5.1.2 Inner cylinder

The temperature distribution along the axis and inner cylinder tells the whole story of heat transfer in such enclosures. The experimental and the CFD results for axial temperature along the inner side of inner cylinder are shown in Figure 6. Figure 6 (a-b) shows the axial temperature distribution along the inner cylinder, using inner cylinder made of aluminum material, under the bottom disc central temperature of 393 K and using two different mild steel outer cylinders O_1 and O_2 . It is observed that the axial temperature distribution along the inner cylinder is independent of the outer cylinder diameter.

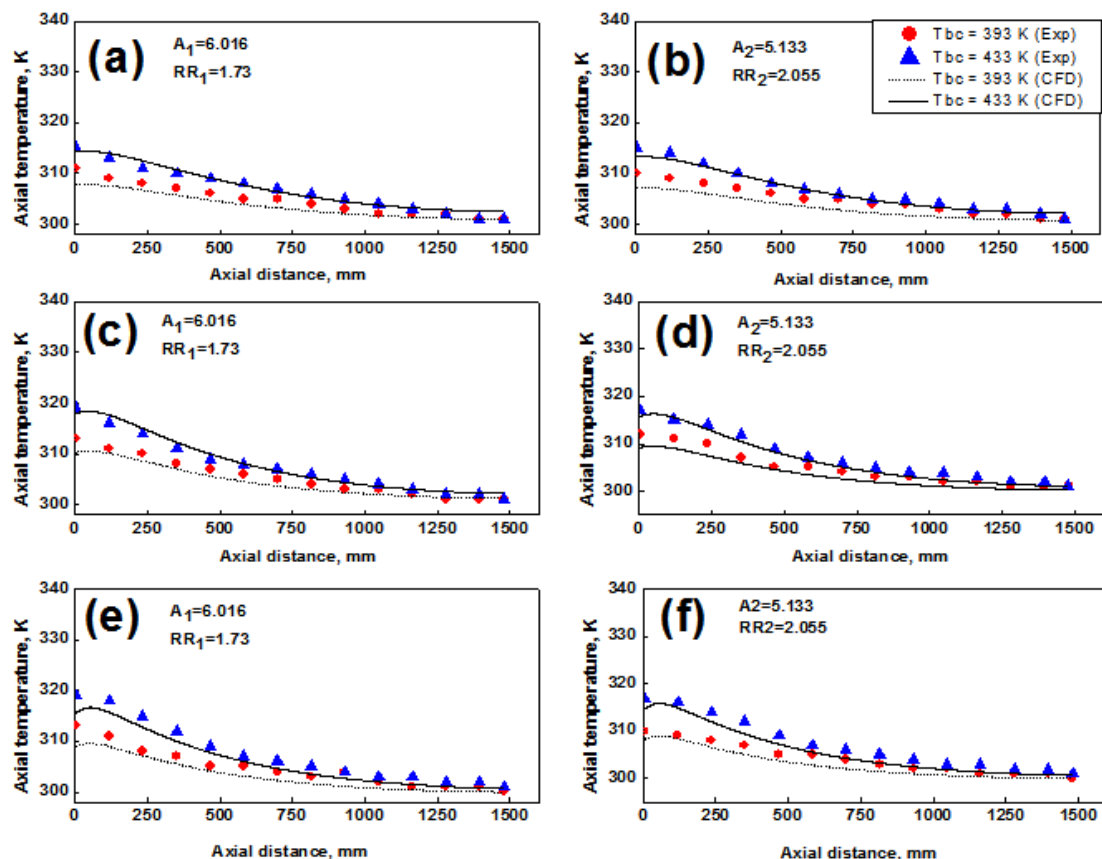


Figure 6: Axial temperature along the inner surface of inner cylinder of aluminum (a, b), mild steel (c, d) and stainless steel (e, f)

Figure 6 (c-d) and Figure 6 (e-f) show the same results using inner cylinders of mild steel and stainless steel respectively. It is observed that the axial temperature along the inner cylinder depends on the diameter of the outer cylinder.

Due to higher thermal conductivity of aluminum the heat is transferred easily to the outer enclosure irrespective of the diameter of the outer cylinder. While, in the case of mild steel and stainless steel inner cylinders the thermal conductivities of the inner cylinder are low and therefore the axial temperature along the inner cylinder is a function of the diameter of the outer cylinder as well. The spread in temperature distribution for various bottom disc temperatures is more in Figure 6 (c-f) as compared to Figure 6 (a-b). The reason might be due to higher thermal conductivity of aluminum as compared to mild steel and stainless steel. The close agreement between the experimental and the CFD results of axial temperature along inner cylinder support the numerical simulation of vertical concentric cylindrical enclosure.

5.2 Validation of the CFD simulation

Before discussing the CFD results an effort is made to validate the CFD simulations. The experimental data of six different experiments are used to validate the CFD results using aluminum, mild steel and stainless steel inner cylinders in the experiments. The CFD and experimental results have been compared in the following sections.

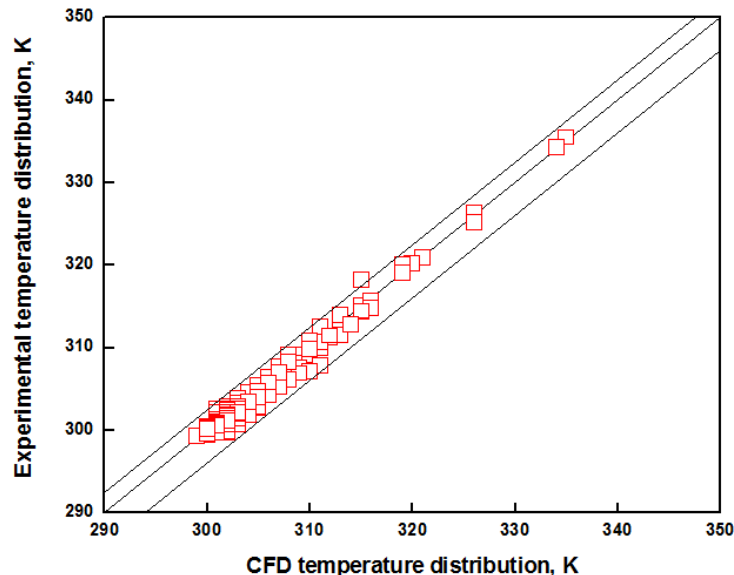


Figure 7: Comparison of experimental and the CFD results of enclosure with aluminum inner cylinder

The comparison of experimental results with the CFD simulation results of enclosure configurations (O_1 , O_2) at different bottom disc central temperatures (353, 393 and 433 K) have been shown in Figure 7. The positive and negative errors of the CFD simulation results with the experimental ones are 0.8% and 1.3% respectively (Figure 7). This shows that the CFD simulation results are in best agreement with experimental ones. Hence, the CFD simulation results of enclosure configurations (O_1 , O_2) with aluminum inner cylinder at different bottom disc central temperatures (353, 393 and 433 K) are validated with the experimental results.

5.3 The CFD simulation results

In order to study the heat transfer mechanism and buoyancy effects in vertical concentric cylindrical enclosure in more depth CFD results have been discussed in the following sections.

5.3.1 Contours of streamlines at 393 K

The contours of streamlines are obtained from CFD simulations for the enclosure configurations O_1 and O_2 at bottom disc central temperature of 393 K and are shown in Figure 8. Figure 8 (a-b) shows streamlines for two configurations (O_1 , O_2) of aluminum inner cylinder. Similarly Figures 8 (c-d) and (e-f) show the corresponding results for mild steel and stainless steel inner cylinders. It is observed in Figure 8 (a-b) that the streamlines within the inner cylinder are same for both configurations (O_1 , O_2) of aluminum inner cylinder. The same behavior is observed in case of mild steel (Figure 8 (c-d)) and

stainless steel inner cylinders (Figure 8 (e-f)). The streamlines in the inner cylinder of Figure 8 (a-b) shows weak buoyancy effects as compared to Figure 8 (c-f). The buoyancy effects are stronger in the outer annulus with outer cylinder configuration O_2 as compared to configuration O_1 for all three inner cylinders used. The buoyancy effects in the outer annulus are stronger in case of aluminum inner cylinder as compared to mild steel and stainless steel for the same outer configuration. The same behavior is observed in case of mild steel inner cylinder as compared to stainless steel. At this temperature the heat added to the enclosure is small and buoyancy effects are relatively weak in Figure 8 (a-b) as compared to Figure 8 (c-f) due to difference of thermal conductivity.

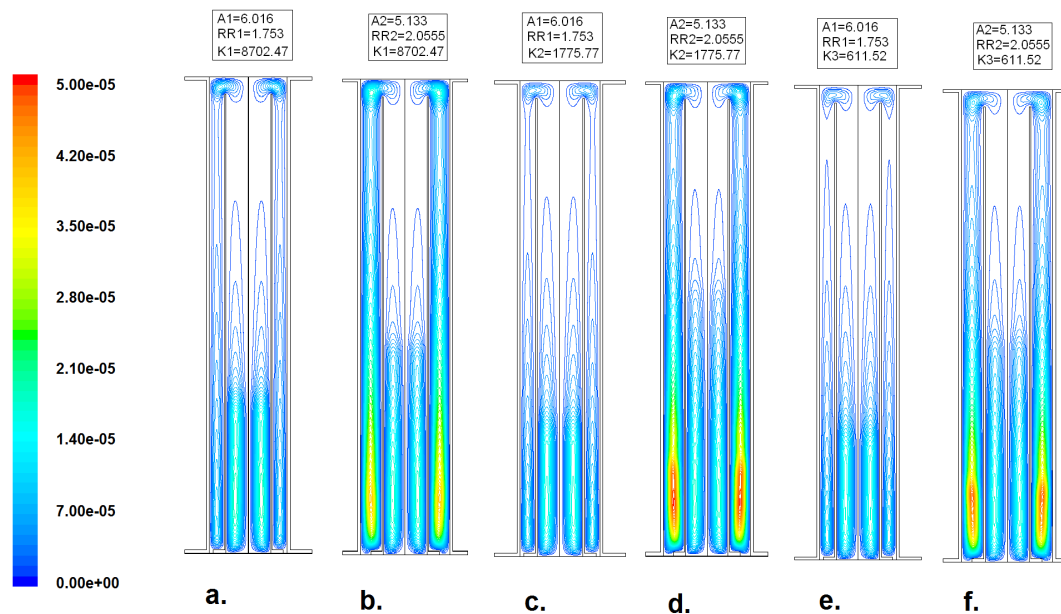


Figure 8: Streamlines of enclosure for configuration O_1 inner cylinders of a). aluminum, c). mild steel, e). stainless steel, for configuration O_2 inner cylinders of b). aluminum, mild steel, f). stainless steel at 393 K.

Due to increase in volume of outer cylinder configuration O_2 the buoyancy effects are stronger as compared to configuration O_1 . In the outer annulus the buoyancy effects are stronger while using inner cylinder of aluminum as compared to other inner cylinders due to its high thermal conductivity.

5.3.2 Comparison of contours of streamlines

At a bottom disc central temperature of 433 K the buoyancy effects are stronger [35] as compared to the buoyancy effects at 393 K for all three inner cylinders used. At 433 K the outer cylinder diameter also affects the heat transfer mechanism within the inner cylinder due to large quantity of heat transfer through the enclosure due to increase in volume as compared to configuration O_1 for three inner cylinders used while comparing the same streamlines at 393 K.

The stream lines at 393 K and 433 K suggest that due to high thermal conductivity of aluminum inner cylinder, the heat conduction in inner cylinder wall in the axial direction is high as compared to inner cylinders of mild steel and stainless steel. This behavior is more clearly visible at 433 K, where due to low thermal conductivity of mild steel and stainless steel double vortices are formed in the outer annulus region with outer cylinder configuration O_2 .

6. Conclusion

In this study the CFD analysis of conjugate heat transfer within a bottom heated non-conventional cylindrical enclosure is performed. Thermal lines, streamlines and velocity vectors of the enclosure

are studied at bottom disc temperature of 393K for the inner cylinder material (aluminum, mild steel, stainless steel) and outer cylinder diameter (O_1 , O_2). In total six different simulations are performed. As a result of these experiments following conclusions are made;

1. A more uniform axial temperature is seen at the inner wall of aluminum cylinder at a bottom disc temperature of 393K and outer cylinder diameters (O_1 , O_2) as compared to mild steel and stainless steel.
2. Stainless steel is more sensitive to outer cylinder diameter as compared to mild steel. Here, the outer cylinder diameter is the controlling parameter for the heat transfer mechanism rather along with the thermal conductivity. Aluminum is non-sensitive to the outer cylinder diameters (O_1 , O_2) specifically for the inner cylinder thermal behavior.
3. In mild steel and stainless steel inner cylinders the temperature spread near the bottom disc at a temperature of the bottom disc 393K decreases with increasing outer cylinder diameters.
4. At the bottom disc temperature up to 393 K the streamlines within the inner cylinder are almost same for both configurations (O_1 , O_2) of three inner cylinders of aluminum, mild steel and stainless steel being independent of outer diameter used.
5. Buoyancy effects are more prominent in the aluminum inner cylinder as compared to the mild steel and stainless steel inner cylinders showing its convection effects.
6. With outer cylinder configuration O_2 the buoyancy effects are stronger due to increase in volume as compared to configuration O_1 for three inner cylinders used.
7. In the outer annulus the buoyancy effects are stronger while using inner cylinder of aluminum as compared to other inner cylinders due to its high thermal conductivity.
8. With the increase in temperature from 393 K to 433 K the heat conduction in inner cylinder wall in the axial direction is high and more visible as compared to inner cylinders of mild steel and stainless steel due to high thermal conductivity of aluminum inner cylinder.

References

- [1]. Lemembre, A.a.P., J. P., *Laminar Natural Convection in a Laterally Heated and Upper Cooled Vertical Cylindrical Enclosure*. International Journal of Heat and Mass Transfer, 1998. 41(16): p. 2437-2454.
- [2]. Chen, S.A.H., J. R., Humphrey, J. A. C. , *Steady, Two-Dimensional, Natural Convection in Rectangular Enclosures With Differently Heated Walls* Journal of Heat Transfer, Transactions of the ASME, May 1987. 109: p. 400-406.
- [3]. Sharma, A.K., Velusamy, K. and Balaji, C., *Conjugate Transient Natural Convection in a Cylindrical Enclosure with Internal Volumetric Heat Generation* Annals of Nuclear Energy, 2008. 35: p. 1502-1514.
- [4]. Franke, M.E. and K.E. Hutson, *Effects of Corona Discharge on Free-Convection Heat Transfer Inside a Vertical Hollow Cylinder*. Journal of Heat Transfer, 1984. 106(2): p. 346-351.
- [5]. Roschina, N.A., Uvarov, A. V. and Osipov, A. I., *Natural Convection in an Annulus Between Coaxial Horizontal Cylinders with Internal Heat Generation*. International Journal of Heat and Mass Transfer October 2005. 48(21-22): p. 4518-4525.
- [6]. Bairi, A., *Transient Natural 2D Convection in a Cylindrical Cavity with the Upper Face Cooled by Thermoelectric Peltier Effect Following an Exponential Law* Applied Thermal Engineering, March 2003. 23(4): p. 431-447.
- [7]. Kim, D.M.a.V., R., *Effect of Wall Heat Conduction on Natural Convection Heat Transfer in a Square Enclosure*. Journal of Heat Transfer, Transactions of the ASME, February 1985. 107: p. 139-146.
- [8]. Vargas, M., Sierra, F. Z., Ramos, E., and Avramenko, A. A., *Steady Natural Convection in a Cylindrical Cavity*, . International Communication of Heat and Mass Transfer, 2002. 29(2): p. 213-221.

- [9]. Kee, R.J., Landram, C. S. and Miles, J. C., *Natural Convection of a Heat Generating Fluid within Closed Vertical Cylinders and Spheres* Journal of Heat Transfer, Transactions of the ASME, February 1976. 98(1): p. 55-61.
- [10]. Bohn, M.S.a.A., R., *Temperature and Heat Flux Distribution in a Natural Convection Enclosure Flow*. Journal of Heat Transfer, Transactions of the ASME, May 1986. 108: p. 471-476.
- [11]. Liaqat, A.a.B., A. C., *Conjugate Natural Convection in a Square Enclosure Containing Volumetric Sources* International Journal of Heat and Mass Transfer, September 2001. 44(17): p. 3273-3280.
- [12]. Kuznetsov, C.V.a.S., M. A., *Conjugate Heat Transfer in an Enclosure under the Condition of Internal Mass Transfer and in the Presence of the Local Heat Source*, . International Journal of Heat and Mass Transfer, 2009. 52: p. 1-8.
- [13]. Glakpe, E.K., Watkins, C.B. and Kurien, B.J., *Effect of Radiation and Specified Heat Flux on Natural Convection in a Vertical Region with a Rectangular Inner Boundary*, . AIAA and ASME, Joint Thermodynamics and Heat Transfer Conferences, 4th Boston, M.A. , June 2-4, 1986: p. 10 pages.
- [14]. Malik, A.H., et al., *Experimental Study of Conjugate Heat Transfer within a Bottom Heated Vertical Concentric Cylindrical Enclosure*. International Journal of Heat and Mass Transfer, 2012. 55: p. 1154-1163.
- [15]. Fluent, *Fluent 6.3 User's Guide*. Fluent Inc., 2006.
- [16]. Rolf H. Sabersky, A.J.A., Edward G. Hauptmann, *Fluid Flow - A First Course in Fluid Mechanics*. Macmillan Publishing Co., Inc., New York, Collier Macmillan Publishers, London, 1971. Second Edition.
- [17]. White, F.M., *Fluid Mechanics*. 1986. Second Edition.
- [18]. Robert L. Daugherty, J.B.F.a.E.J.F., *Fluid Mechanics with Engineering Applications*. McGraw Hill Book Company, Singapore, 1996. S. I. Metric Edition.
- [19]. Wrobel, W., Fornalik-Wajs, E., and Szmyd, J. S., *Experimental and Numerical Analysis of Thermo-magnetic Convection in a Vertical Annular Enclosure*, . International Journal of Heat and Fluid Flow, December 2010, 31(6): p. 1019-1031.
- [20]. Covaro, F.a.P., Massimo *The Natural Convective Heat Transfer in a Partially Divided Enclosure: A study on the Influence of the Source Position*. Journal of Thermodynamics, 2009, 2009: p. 1-11.
- [21]. Kuznetsov, G.V.a.S., Mikhail A., *Conjugate Natural Convection in an Enclosure with a Heat Source of Constant Heat Transfer Rate* International Journal of Heat and Mass Transfer, January 2011. 54(1-3): p. 260-268.
- [22]. Aminossadati, S.M.a.G., B., *The Effects of Orientation of an Inclined Enclosure on Laminar Natural Convection* Heat and Technology, 2005. 23(2): p. 43-49.
- [23]. Nazrul Islam, G., U.N., and Sharma, G.K., *Mixed Convection Heat Transfer in the Entrance Region of Horizontal Annuli* International Journal of Heat and Mass Transfer, June 2001. 44(11): p. 2107-2120.
- [24]. Sezai, I.a.M.A.A., *Natural Convection Heat Transfer from a Discrete Heat Source on the Bottom of a Horizontal Enclosure* International Journal of Heat and Mass Transfer, 2000. 43: p. 2257-2266.
- [25]. Mazumder, S., *On the Use of the Fully Compressible Navier Stokes Equations for the Steady-State Solution of Natural Convection Problems in Closed Cavities* Journal of Heat Transfer, Transactions of the ASME, March 2007. 129: p. 387-390.
- [26]. Bouali, H., Mezrhab, A., Amouli, H. and Bouzidi, M., *Radiation – Natural Convection Heat Transfer in an Inclined Rectangular Enclosure* International Journal of Thermal Sciences, 2006. 45: p. 553-566.
- [27]. Yu, E.a.J., Y.K., *Heat Transfer in Discretely Heated Side-Vented Compact Enclosures by Combined Conduction, Natural Convection and Radiation* Journal of Heat Transfer, Transactions of the ASME, November 1999. 121: p. 1002-1010.
- [28]. Chang, T.S.a.T., Y.L., *Natural Convection Heat Transfer in an Enclosure with a Heated Background Step*, . International Journal of Heat and Mass Transfer, 2001. 44: p. 3963-3971.

- [29]. Zhao, F.-Y., Liu, Di and Tang, Guang-Fa, *Natural Convection in an Enclosure with Localized Heating and Salting from Below* International Journal of Heat and Mass Transfer, 2008. 51: p. 2889-2904.
- [30]. Lin, W.a.A., S. W., *Natural Convection Cooling of Rectangular and Cylindrical Containers*, . International Journal of Heat and Fluid Flow 2001. 22: p. 72-81.
- [31]. Papanicolaou, E.a.B., V., *Transient Natural Convection in a Cylindrical Enclosure at High Rayleigh Numbers* International Journal of Heat and Mass Transfer, March 2002. 45(7): p. 1425-1444.
- [32]. Khalilollahi, A.a.S., B., *Unsteady Natural Convection Generated by a Heated Surface Within an Enclosure* Numerical Heat Transfer, 1986. 9: p. 715-730.
- [33]. Cengel, Y.A., *Heat Transfer a Practical Approach*. McGraw Hill Companies, Inc, 1221 Avenue of the Americas, New York, 2003. Second edition.
- [34]. Moffat, R.J., *Contributions to the Theory of Single-Sample Uncertainty Analysis*. Journal of Fluids Engineering, 1982. 104(2): p. 250-258.
- [35]. Malik A. H., e.a., *Numerical Study of Conjugate Heat Transfer within a Bottom Heated Cylindrical Enclosure*. Proceedings of 2012, 9th International Bhurban Conference on Applied Sciences & Technology (IBCAST), Islamabad, Pakistan, 9-12 January, 2012: p. 213-220.